applied sciences

MDPI

Article

Establishment of a Novel Fragmentation Prediction Model Incorporating Rock's Response Time to Blasting

Meric Can Ozyurt [1], Abdulkadir Karadogan [1,*], Ulku Kalayci Sahinoglu [1], Umit Ozer [1], Hilal Erem Mutlu [2] and Taki Can Odabasi [3]

[1] Mining Engineering Department, Engineering Faculty, Istanbul University-Cerrahpasa, 34500 Istanbul, Türkiye; meric.ozyurt@iuc.edu.tr (M.C.O.); ukalayci@iuc.edu.tr (U.K.S.); uozer@iuc.edu.tr (U.O.)
[2] Tessan Mining Construction Industry Tourism and Trade Joint Stock Company, 34076 Istanbul, Türkiye; hilalerem0912@gmail.com
[3] Erdemir Mining Industry and Trade Inc., 58300 Divrigi, Türkiye; takicanodabasi@gmail.com
* Correspondence: akadir@iuc.edu.tr

Abstract

Rock's response time to blasting (T_{min}) refers to the critical time elapsed between the detonation of the explosive to the fragmentation and displacement of the rock, and it is a fundamental parameter that directly impacts blast-induced fragmentation. Although existing studies acknowledge the importance of this parameter, there are uncertainties regarding the factors determining T_{min}. Furthermore, existing models use complex parameters, fail to demonstrate sufficient performance in different engineering scenarios, or are not suitable for use as a practical engineering tool. To address these uncertainties and to reveal the relationship between T_{min} and fragmentation performance with an integrated model, a comprehensive dataset was obtained from 27 blasts conducted in 12 different quarries in Türkiye. The study followed a systematic methodology including geomechanical characterization, T_{min} measurement via high-speed videography, and pre- and post-blast photogrammetric fragment size analysis. The findings enabled the development of a model that predicts T_{min} with high accuracy (R^2 = 0.789, MAPE: %16.56) using parameters easily measurable in practice. More importantly, this estimation of T_{min} was used in an integrated model where the mean fragment size (P_{50}) could be predicted directly and successfully (R^2 = 0.837, MAPE: %8.37), providing a significant contribution to the literature. In light of these results, the primary engineering contribution of the study is that it has developed a practical and reliable tool applicable in the field, which treats T_{min} as an optimizable design variable and provides a seamless prediction framework from blasting design to the rock fragmentation.

Keywords: blasting; rock fragmentation; rock's response to blasting; rock movement; high speed video records

check for updates

Academic Editor: Ricardo Castedo

Received: 11 August 2025
Revised: 23 August 2025
Accepted: 27 August 2025
Published: 28 August 2025

Citation: Ozyurt, M.C.; Karadogan, A.; Kalayci Sahinoglu, U.; Ozer, U.; Mutlu, H.E.; Odabasi, T.C. Establishment of a Novel Fragmentation Prediction Model Incorporating Rock's Response Time to Blasting. *Appl. Sci.* **2025**, *15*, 9447. https://doi.org/10.3390/app15179447

Correction Statement: This article has been republished with a minor change. The change does not affect the scientific content of the article and further details are available within the backmatter of the website version of this article.

Copyright: © 2025 by the authors. Licensee MDPI, Basel, Switzerland. This article is an open access article distributed under the terms and conditions of the Creative Commons Attribution (CC BY) license (https://creativecommons.org/licenses/by/4.0/).

1. Introduction

Blasting is a fundamental method used for the fragmentation of hard rocks. The foundation of this technique is the controlled detonation of explosive materials inserted into holes drilled into the rock mass, followed by using the blasting energy released to fragment the rock to the required size.

The fragmentation mechanism that underlies this controlled fragmentation is a sequence of sequential reactions that starts with the initiation of the explosive charge. Upon

the detonation of the explosive charge, the suddenly released gases at very high temperature and pressure strike the borehole walls, creating an intense pressure wave that propagates outwards through the rock. This stress wave from the blast exceeds the rock's stress strength in a very short time, shattering and breaking the region immediately surrounding the hole and creating a zone that has been plastified and pulverized into dust. Outside this zone, plastic behavior transitions to elastic behavior, forming a fractured zone. The tangential (tensile) stresses generated here cause the formation of cracks that propagate in a radial direction. The radial cracks continue to propagate until the tangential tensile stress falls below the tensile strength of the rock. When the released radial pressure waves hit a free surface, they reflect and transform into tensile stress waves. These reflected tensile waves advance the fracturing initiated around the hole, triggering the formation of radial cracks extending to distances up to four times the borehole diameter. Subsequently, the high-pressure gases penetrate these radial cracks, pushing them like a wedge and propelling the cracks all the way to the free surface, thereby achieving the final fragmentation of the rock. In the final stage, the same gas pressure displaces the fragmented rock mass, completing the blasting cycle [1–7]. This entire duration, from the detonation of the explosive to the fragmentation and displacement of the rock, was defined by Chiappetta [8] as the rock's response time to blasting (T_{min}).

Since its discovery, rock fragmentation by blasting has attracted substantial research interest aimed at enhancing fragmentation performance. The primary challenge in achieving desired fragment size distribution lies in rock inhomogeneity and the complex interplay of stress wave propagation and gas penetration mechanisms. Consequently, determining site-specific blasting parameters tailored to each geological environment remains essential. While specific charge optimization through hole pattern and charge amount adjustments is commonly employed, numerous studies have demonstrated that delay timing constitutes an equally critical parameter for fragmentation control. Research shows optimal delay times range from 3 to 8 ms/m of burden [9–13] to 10 ms/m [14], with consistent findings indicating improved fragmentation at delays exceeding 3.3 ms/m and deterioration below 1 ms/m [15,16]. Some researchers propose spacing rather than burden as the key parameter [17,18], with detailed rock-specific recommendations available [17]. Empirical studies confirm that increased delay times up to 11–13 ms/m generally reduce mean fragment size and improve fragmentation efficiency [19–21], though excessively long delays may diminish effectiveness due to loss of stress wave interaction.

As mentioned above, various studies and suggestions have been put forward for the ideal delay interval to achieve good fragmentation. However, guidelines often require adaptation and may not be directly transferable to all field conditions, largely due to the unpredictable nature of blasting and the significant inhomogeneity inherent to rock units. Well aware of this complexity, Jimeno et al. [5], emphasized that delay timing should enable the total completion time of the sequence of events that comprise the rock fragmentation mechanism by blasting, rather than recommending definitive numerical values. This perspective—which refers to the duration of sequential reactions from explosive initiation to rock fragmentation and displacement, or the rock's response time to blasting in Chiappetta [8] terms—has shed important light on the field by suggesting that such timing may play a critical role in achieving optimal fragmentation. Nevertheless, the number of scientific studies that have examined its impact on fragmentation performance is considerably limited.

The term "rock's response time to blasting" was first defined by Chiappetta [8], and it depends on the burden/hole diameter ratio. For good results in rock fragmentation, the delay time between holes in a row should be less than or equal to T_{min}, and the delay time

between rows should be 1.5–3 times T_{min}. Depending on the blasted material, T_{min} varies from a few milliseconds to hundreds of milliseconds.

Onederra and Esen [22] developed an empirical complex model, introducing new parameters such as rock hardness (K_{mass}) and explosive–rock interaction (ERI) (Equation (1)).

$$T_{min} = (K_{mass} \times ERI)\left[a \times \left(\frac{B}{d} \times \left(\frac{1}{K_{mass} \times ERI}\right)\right)^{b}\right] \quad (1)$$

where T_{min} is the minimum response time (ms); K_{mass} is the rock mass stiffness (GPa) which is a function of the rock mass dynamic Young's modulus (E_d) and Poisson's ratio (v_d); B is the burden (m); d is the hole diameter (m) and ERI is an explosive rock interaction term. While K_{mass} is calculated by using Equation (2), the term ERI is determined by Bergmann [4] formula (Equation (3)).

$$K_{mass} = \frac{E_d}{(1 + v_d)} \quad (2)$$

$$ERI = (0.36 + \rho_e) \times \left(\frac{D^2}{(1 + \frac{D^2}{v_p^2} - \frac{D}{v_P})}\right) \times \left(\frac{D}{D_{cj}}\right) \times \rho_e \quad (3)$$

where ERI is the explosive–rock interaction term; ρ_e is the density of the explosive (g/cm^3); D is the actual (non-ideal) detonation velocity (km/s); v_p is the P–wave velocity of the intact rock (km/s) and D_{CJ} is the C_J detonation velocity (km/s).

Segarra et al. [23] and Sanchidrián et al. [24] proposed a contrasting perspective, suggesting that parameters such as rock type and bench height exhibit negligible influence on T_{min}. Their model posits that T_{min} demonstrates an inverse functional relationship solely with burden, representing a significant departure from other theoretical frameworks in the literature.

Onederra [25] continued the work performed by Onederra and Esen [22] and made empirical graphs that will help determine delay duration under different conditions.

Voulgarakis et al. [26] conducted a pioneering and, to our knowledge, the sole study that explicitly quantified the relationship between rock fragmentation and T_{min} using dimensional analysis, introducing a definitive mathematical formulation for this relationship (Equation (4)).

$$T_{min} = \left[\frac{0.077 \times M_0 \times B_L^2}{(7.116 - RR_{50}) \times E_r}\right]^{1/2} \quad (4)$$

where T_{min} is the minimum response time, M_0 is the mass of blasted rock, B_L is the local burden, RR_{50} is the fragmentation ratio and E_r is the released explosive energy.

As mentioned above, researchers widely acknowledge the critical importance of the T_{min} for fragmentation quality and blasting efficiency. Experimental studies confirm the fragmentation mechanism involves sequential reactions, requiring precise timing. However, significant disagreement persists regarding the specific parameters determining this precise timing (T_{min}) and its calculation, highlighting the subject's complexity.

While a strong theoretical foundation exists, a clear need remains for translating these models into practical tools for engineers. The negative influence of burden is well-documented, but the combined effects of other parameters require refinement for better field accuracy. Furthermore, developing a verified, comprehensive calculation tool for direct on-site use is an area for advancement, necessitating a stronger experimental emphasis on the T_{min}-fragmentation correlation.

The conflicting literature provides a strong rationale for this subject and study aims to address these gaps. The primary engineering objective is to develop a comprehensive and

T_{min}-integrated predictive model for fragmentation by blasting. Unlike existing approaches, this research was designed to extend beyond predicting T_{min} by utilizing this parameter as a direct input to sequentially estimate rock-size reduction ratio (F, %) and ultimately the mean particle size (P_{50}). Thus, this study is the first in the literature to establish a novel model that directly integrates the prediction of T_{min} with the estimation of P_{50}.

The study employed a sequential methodology (Figure 1): (1) Characterizing field geology and quantifying rock mechanical properties. (2) Pre-blast studies included meticulous measurement of blast design parameters, detonator timing verification, and photogrammetric quantification of in situ block size distribution on bench faces with Split Desktop v2.0 from Split Engineering, USA. (3) Blast monitoring used high-speed videography (1000 fps) Blaster's Ranger II High Speed Camera from MREL, Canada to record detonator initiation (t_0) and rock displacement onset (t_{rm}), enabling calculation of T_{min}. (4) Post-blast studies quantified particle size distribution via photogrammetric assessment of muck piles with Split Desktop v2.0 from Split Engineering, USA, enabling evaluation of fragmentation efficiency against initial block size. (5) Statistical analysis of the data produced in the previous phases by using IBM SPSS Statistics 25 from the IBM Corporation, USA.

2. Study Fields

This study investigates 27 blasts across 12 quarries in Istanbul, Tekirdağ, and Kırklareli in Türkiye (Table 1). The lithological units and geology were systematically determined in the field using geotechnical information forms. The quarries covered by the study contain the four most common rock types encountered in quarrying: limestone, sandstone, marl, and claystone. This lithological diversity encompasses the rock types found in the majority of limestone quarries worldwide.

Table 1. Geological and mechanical characteristics of the study fields.

No	Adress	Formation	Unit	UCS * (MPa)	Rock Classification **	ρ * (t/m^3)	D *** (Mm) Min.	D *** (Mm) Mean (D_{50})	D *** (Mm) Max.
1	Kirklareli	Pinarhisar	Limestone	89	Strong	2.54	1030	2515	5635
2	Kirklareli	Pinarhisar	Limestone	98	Strong	2.52	930	3355	7520
3	Kirklareli	Pinarhisar	Limestone	71	Strong	2.52	755	3665	4690
4	Kirklareli	Suloglu	Sandstone	95	Strong	2.55	365	3600	1865
5	Kirklareli	Sogucak	Limestone	48	Strong	2.50	520	3430	2960
6	Kirklareli	Sogucak	Limestone	42	Strong	2.44	1580	2705	4970
7	Kirklareli	Thrace	Limestone	76	Strong	2.51	310	1925	3395
8	Kirklareli	Suloglu	Sandstone	55	Strong	2.50	330	1660	3200
9	Kirklareli	Islambeyli	Marn	130	Very Strong	2.55	310	2170	4360
10	Istanbul	Thrace	Sandstone	126	Very Strong	2.54	420	2110	3930
11	Kirklareli	Suloglu	Limestone	186	Very Strong	2.60	1430	1990	6135
12	Tekirdag	Danismen	Claystone	37	Moderate	2.50	860	1820	5025

UCS: Uniaxial Compressive Strength, ρ: Unit Volume Weight of the Rock, D: In Situ Block Size, * Obtained from laboratory test performed on samples taken from blasted rock, ** Classification based on uniaxial compressive strength values, *** Determined through photogrammetric quantification of in situ block size distribution on bench faces.

Subsequently, laboratory testing of representative rock samples was conducted to quantify *UCS* and ρ. In terms of rock strength, the study encompasses a wide range of samples, from moderate strong to very strong, where blasting is technically and economically necessary. Similar variability was also observed in discontinuity networks that regulated in situ block sizes.

Despite the geographical limitations, considering the lithological diversity, rock strength range, and industrial application criteria covered by the study, it can be said that the study fields are representative of quarries on a global scale. In addition, this diversity enables the development of generalized predictive models that can be applied in

various geological contexts, thereby enhancing our understanding of the rocks' response time to blasting.

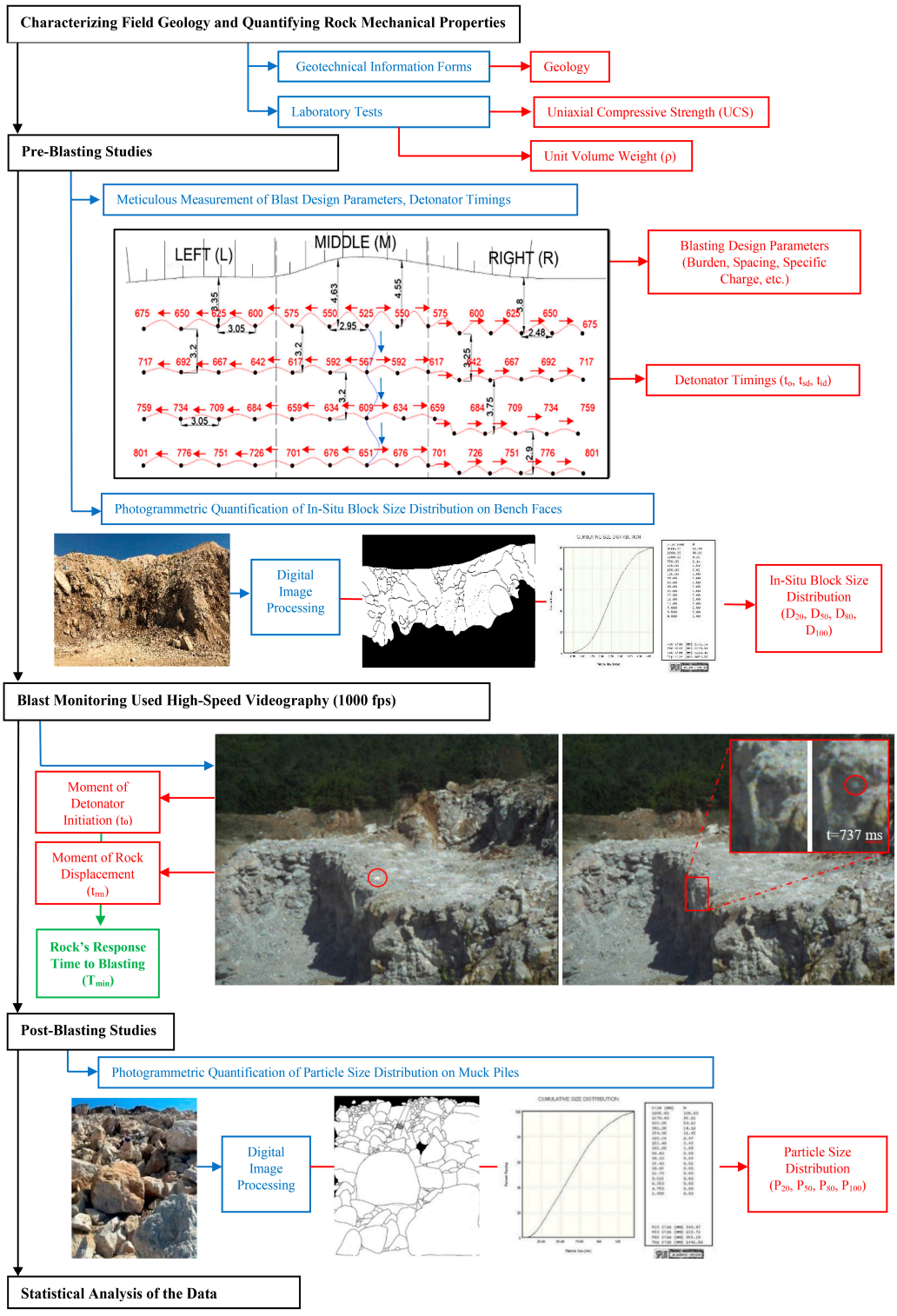


Figure 1. Schematic representation of the methodological approach used in the study.

2.1. Danismen Formation

The Danismen formation is of Late Oligocene—Early Miocene age. The formation consists of greenish gray shales, clay stones and coals which are interbedded with light gray to yellowish brown and cross-bedded, fine-grained sandstones and siltstones [27].

2.2. Islambeyli Formation

The Islambeyli Formation, with a thickness varying between 30 and 100 m, is overlain by the Kirklareli Limestone via both lateral and vertical transitions. The formation begins with a basal sediment of weakly compacted, poorly sorted, angular, blocky, pebble- to sand-sized volcaniclastic sandstone-conglomerate. This is overlain by a hard, tightly compacted succession of sandstone, claystone, marl, and limestone with yellow to off-white-gray carbonate cement. The unit also contains tuffs and tuffites exhibiting convolute structures, which are interbedded with locally gray and greenish marls [28,29].

2.3. Thrace Formation

The dominant units in the region are claystones and sandstones. Sediments generally show a stratified structure, and faults and compression zones are encountered in some places. For this reason, crushed, cracked, and folded structures are frequently encountered in the quarry [30].

2.4. Pinarhisar Formation

The Pınarhisar Formation, composed of sandstone, pebbly sandstone, conglomerate, and various oolitic and clayey limestones, is widely accepted to lie on the eastern shore of the Thrace Basin, though its age and correlations remain debated. It transitionally overlies the Kırklareli Limestone toward the basin center but rests unconformably upon the basin-equivalent Soğucak Formation along the northern margin due to active tectonism. The gray to dun-colored unit includes thin to medium beds of quartz and limestone pebbles, oolitic coatings, and layers rich in gastropod and lamellibranch shells, grading upward into manganese-bearing sandstones, angular conglomerates, and oolitic limestones containing fish teeth. It is broadly considered to be of Oligocene age [31,32].

2.5. Sogucak Formation

The age of the Sogucak formation varies from Late Lutetian to Early Oligocene along the basin [33]. The Sogucak formation overlies the Koyunbaba formation in the northern Thrace Basin with a gradual transition. The depositional environments of the Soğucak Formation can be defined as shallow marine to deep open marine environments [34].

2.6. Suloglu Formation

The Sogucak Formation consists of gray to beige, thin-bedded, slightly carbonaceous shales and siltstones with fish fossils at the base, transitioning upward into yellowish-gray sandstones and greenish-gray claystones. The sandstones are locally tight-bonded, thin- to medium-bedded, and medium- to coarse-grained, while the claystones are massive and greenish in appearance. The unit contains lignite bands, particularly in the west near the metamorphic basement, as well as vertically bedded manganese levels and sandstones toward its base. Its coal-bearing sandy upper sections are partially correlated with the Danismen Formation. The age of the unit is considered Middle to Late Oligocene [35].

3. Field Studies

3.1. Blasting Design Parameters

As part of the pre-blast studies, hole design for each shot were meticulously measured using calibrated tape measures, while detonator connections were inspected to ensure millisecond-level timings. Due to significant variability in field-measured parameters—including in situ block size, hole design, and charge distribution—a zone-based analytical framework was implemented to systematically manage variance, as shown in figure under the subheading ‘meticulous measurement of blast design parameters, detonator timings’

in Figure 1. By establishing predefined thresholds for critical blasting parameters, the 27 blasting events were segmented into 51 statistically robust datasets. This methodological refinement effectively mitigated high standard deviations and facilitated the identification of causative relationships between blasting parameters and fragmentation.

Since it is not possible to share all the values of blasting design parameters, pertinent charge specifications, and capsule details from the study, a representative part is presented in Table 2.

Table 2. Representative values of blasting design parameters, pertinent charge specifications, and capsule details.

Field No	Shot No	Zone	B_{max} (m)	S (m)	K (m)	d (mm)	Explosive	I_b (kg/m)	n	U (m)	H (m)	h_o (m)	VoD (m/s)	Q (kg)	q (kg/m^3)	Inter-Hole Delay (ms)	Inter-Row Delay (ms)
1	1	-	3.45	3	9	89	ANFO	4.97	13	2	10	2.8	4905	36.82	0.31	25/500	17
	2	Left	4	3.2	9	89	ANFO	4.97	20	0.5	9.5	2	4905	38.31	0.42	25/500	17
		Middle	3.25	3.05	9	89	ANFO	4.97	20	0.5	9.5	2	4905	38.31	0.39	25/500	17
		Right	2.25	2.47	9	89	ANFO	4.97	20	0.5	9.5	2	4905	38.31	0.45	25/500	17
5	9	Left	2.75	2.7	8	89	ANFO	4.97	43	2	10	2.5	4905	38.31	0.52	25/500	17
		Right	2.9	2.7	8	89	ANFO	4.97	40	2	10	2.5	4905	38.31	0.47	25/500	17
6	10	Left	3.9	2,5	8	89	Emulsion	7.77	25	1	9	3	5450	46.63	0.46	17/500	25
		Right	3.95	2,9	8	89	Emulsion	7.77	20	1	9	3	5450	46.63	0.46	17/500	25
8	12	Left	4.15	4.1	9	102	ANFO	6.53	35	1	10	3	4905	46.74	0.38	25/500	17
		Middle	4.25	3.6	9	102	ANFO	6.53	40	1	10	3	4905	46.74	0.4	25/500	17
		Right	3.35	3.5	9	102	ANFO	6.53	40	1	10	3	4905	46.74	0.46	25/500	17
9	13	Left	3.15	3.3	10	127	ANFO	10.13	44	1	11	3	4830	82.03	0.38	33/500	42
		Right	2.8	3.7	10	127	ANFO	10.13	40	1	11	3	4830	82.03	0.32	33/500	42
	16	Left	2.95	3.4	8	127	ANFO	10.13	36	1	9	3	4830	61.77	0.62	33/500	42
		Right	3.3	3.5	8	127	ANFO	10.13	36	1	9	3	4830	61.77	0.61	33/500	42

B_{max}: Maximum Burden, S: Spacing, K: Bench Height, d: Blasthole Diameter, I_b: Charge Concentration, n: Number of Blastholes, U: Subdrilling Length, H: Blasthole Length, h_o: Stemming Length, VoD: Velocity of Detonation, Q: Total Charge, q: Specific Charge.

3.2. Rock Fragmentation by Blasting

This study quantified the in situ block size distribution on pre-blast bench faces and the particle size distribution of post-blast muck piles using photogrammetry. Representative sections of bench faces and fragmentation zones were systematically photographed under controlled conditions. Subsequent digital image processing characterized the pre-blast in situ block sizes (D_{20}, D_{50}, D_{80}, D_{100}) and post-blast particle size (quantified by P_{20}, P_{50}, P_{80}, P_{100}) by using Split Desktop v2.0.

While the complete dataset exceeds the scope of this study, a statistically representative subset of results (Table 3) validates the methodology's application and robustness.

Critically, fragmentation efficiency was evaluated using the rock-size reduction ratio (F, %), defined as the ratio of the mean post-blast particle size (P_{50}, *mm*) to the mean pre-blast in situ block size (D_{50}, mm) (Equation (5)). Higher F values signify enhanced fragmentation performance.

$$F\ (\%) = 100\ \times \left(1 - \frac{P_{50}}{D_{50}}\right) \tag{5}$$

The study achieved high fragmentation efficiency across all blasts, with rates ranging from 83.02% to 96.47% and averaging 86.76%. These results demonstrate consistently effective size reduction, with some blasts approaching near-perfect fragmentation (96.47%).

3.3. Rock's Response Time to Blasting

In this study, Blaster's Ranger II High Speed Camera operating at 1000 frames per second (fps) were deployed to capture the dynamic response of rocks to blasting. This setup effectively slowed real-time events by a factor of 1000 for detailed analysis (1 ms of actual time = 1 s of footage). Footage from each shot was scrutinized frame-by-frame to record two critical timestamps per blast hole: the initiation of the surface capsules, identified when

a distinct color change (e.g., brightening) of the capsule's pixels as shown in picture (a) under the subheading 'blast monitoring used high-speed videography' in Figure 1, and the first observable rock displacement within the hole's designated impact zone, determined using a pixel displacement threshold as shown in picture (b) under the subheading 'blast monitoring used high-speed videography' in Figure 1.

Table 3. A representative part of fragmentation data.

Field No	Shot No	Zone	q (kg/m^3)	D_{20} (mm)	D_{50} (mm)	D_{80} (mm)	D_{100} (mm)	P_{20} (mm)	P_{50} (mm)	P_{80} (mm)	P_{100} (mm)	F (%)
1	1	-	0.31	1341	1843	2730	3681	139	269	459	777	85.38
	2	Left	0.42	3170	5269	9012	11,761	358	729	1204	1800	86.17
		Middle	0.39	2389	3875	5476	8445	341	634	955	1442	83.65
		Right	0.45	2014	3125	5344	6295	218	450	1157	1625	85.60
5	9	Left	0.52	2025	3293	4935	6790	154	237	332	482	92.80
		Right	0.47	1721	2439	3268	4654	118	227	354	658	90.69
6	10	Left	0.46	2355	4043	5764	8511	90	143	209	330	96.47
		Right	0.46	3003	5143	7257	11,054	118	212	367	644	95.88
8	12	Left	0.38	1509	2452	3681	4952	205	339	545	892	86.19
		Middle	0.4	1921	2971	4902	6386	179	329	514	842	88.93
		Right	0.46	2105	2950	4376	6219	150	303	464	666	89.74
9	13	Left	0.38	1905	3230	4634	6476	206	497	748	1107	84.61
		Right	0.32	1620	2536	4158	4978	189	338	697	890	86.69
	16	Left	0.62	2945	3917	6842	8369	285	468	655	928	88.06
		Right	0.61	3332	4799	6757	10,793	343	556	845	1345	88.41

q: Specific charge, D_N: The in situ block size of the bench face at which N percent of material, P_N: The particle size of the rock fragments at which N percent of material, F: Rock-Size Reduction Ratio.

A critical finding from the analysis revealed consistent deviations in surface capsules delay times. Capsules from identical production lots exhibited variations of 4–12% (mean: 9%) across monitored blasts. However, high-speed camera data alone could not assess in-hole delay deviations, necessitating controlled laboratory tests. These tests confirmed that in-hole detonator deviations closely mirrored those of their paired surface counterparts. Consequently, surface and in-hole delay deviations were deemed equivalent, simplifying blast timing error modeling.

To calculate T_{min}, the duration between the ignition of a surface capsule and the commencement of rock movement within the hole's impact zone was calculated. By subtracting the delay times of the capsules and the time required for the explosive to detonate from this duration, the response time of the rock to blasting can be calculated (Equation (6)). A representative part of the results are shown in Table 4.

$$T_{min} = (t_{rm} - t_o) - \left[(1 \mp k)(t_{sd} + t_{id}) + 1000 \times \frac{h}{VoD}\right] \quad (6)$$

where T_{min} is rock's response time to blasting (ms), t_{rm} is the moment when the rock breaks away from the main mass and begins to move (ms), t_o is the moment when the surface capsule is ignited (ms), k is the deviation in the delay time, t_{sd} is the surface delay time (ms), t_{id} is the in-hole delay time (ms), h is the charge length (m) and VoD is velocity of detonation (m/s).

Table 4. A representative part of the data regarding T_{min}.

Field No	Shot No	Zone	h (m)	VoD (m/sn)	t_{sd} (ms)	t_{id} (ms)	k	$t_{rm}-t_o$	$1000\times\frac{h}{VOD}$	T_{min} (ms)
1	1	-	7.2	4905	25	500	0.12	742	1.47	152.53
	2	Left	7.5	4905	25	500	0.12	738	1.53	148.47
		Middle	7.5	4905	25	500	0.12	727	1.53	137.47
		Right	7.5	4905	25	500	0.12	724	1.53	134.47
5	9	Left	7.5	4905	25	500	0.04	640	1.53	92.47
		Right	7.5	4905	25	500	0.04	646	1.53	98.47
6	10	Left	6	5450	17	500	0.16	712	1.10	26.46
		Right	6	5450	17	500	0.16	711	1.10	25.46
8	12	Left	7	4905	25	500	0.04	636	1.43	88.57
		Middle	7	4905	25	500	0.04	636	1.43	88.57
		Right	7	4905	25	500	0.04	644	1.43	96.57
9	13	Left	8	4830	33	500	0.10	632	1.66	44.04
		Right	8	4830	33	500	0.10	621	1.66	33.04
	16	Left	6	4830	33	500	0.10	627	1.24	39.46
		Right	6	4830	33	500	0.10	621	1.24	33.46

4. Statistical Analysis

Experimental data ranges are consistent with the established blasting guidelines, such as those proposed by Langefors and Kihlström [36], Olofsson [37], and Jimeno et al. [5]. Table 5 delineates the operational ranges of predictor variables, encompassing minimum, mean, and maximum values derived from comprehensive field measurements. These operational ranges represent a primary limitation of the study, as their predictive accuracy is constrained to these specific boundary conditions.

Table 5. The limit values of the predictors within the scope of this study.

	B_{max} (m)	I_b (kg/m)	ρ (t/m^3)	h_o (m)	VoD (m/s)	UCS (MPa)	U (m)	D_{50} (mm)	P_{50} (mm)	q (kg/m^3)	T_{min} (ms)	F (%)
Min.	1.5	3.97	2.44	1.00	4750	37	0	624	92	0.18	32.84	83.02
Mean	3.10	6.59	2.53	2.58	4866	98	0.68	3038	387	0.44	93.36	86.76
Max.	4.85	10.13	2.60	4.00	4905	186	2	6869	832	0.76	183.89	96.47

Quantitative relationships were established by conducting a comprehensive multivariate linear regression analysis on the experimental dataset by using IBM SPSS Statistics 25. Two predictive models were developed: the first model (Equation (6)) characterizes the rock's response time to blasting (T_{min}) as a function of six predictors: stemming length (h_o), velocity of detonation (VoD), burden (B), charge concentration (I_b), and rock's unit volume weight (ρ) and uniaxial compressive strength (UCS). The second model (Equation (7)) predicts the rock-size reduction ratio (F) using specific charge (q), rock's uniaxial compressive strength (UCS) and response time to blasting (T_{min}), and subdrilling length (U).

4.1. Rock's Response Time to Blasting (T_{min}) Model

For the T_{min} model, regression diagnostics indicated substantial explanatory power (R^2 = 0.789). Table 6 presents the model summary statistics, and Table 7 presents the analysis of variance (ANOVA), which shows statistical significance at the 95% confidence level ($p < 0.001$). The accompanying coefficients table contains information on the regression coefficients, including standardized beta weights and significance values.

Table 6. Model summary of T_{min} estimation.

Model	R	R Square	Adjusted R Square	Std. Error
1	0.888 [a]	0.789	0.760	20.34720

[a]. Predictors: (Constant) UCS, h_o, VoD, B, I_b, ρ.

Table 7. Analysis of variance for T_{min} estimation.

Model		Sum of Squares	df	Mean Square	F	Sig.
1	Regression	68,075.908	6	11,345.985	27.405	<0.001 [b]
	Residual	18,216.373	44	414.008		
	Total	86,292.280	50			

Coefficients [a]

Model		Unstandardized Coefficients		Standardized Coefficients	t	Sig.
		B	Std. Error	Beta		
1	(Constant)	−1837.383	586.365		−3.134	0.003
	B (m)	18.851	4.222	0.339	4.465	0.000
	I_b (kg/m)	−9.507	1.750	−0.524	−5.432	0.001
	ρ (kg/m^3)	2495.127	379.389	1.631	6.577	0.002
	h_o (m)	−21.917	5.653	−0.319	−3.877	0.001
	VoD (m/ms)	−0.839	0.154	−0.887	−5.467	0.003
	UCS (MPa)	−2.425	0.342	−1.971	−7.091	0.001

[a] Dependent Variable: T_{min} (ms). [b] Predictors: UCS (MPa), h_o (m), VoD (m/ms), [b] (m), I_b (kg/m), ρ (kg/m^3).

The resultant regression equation for T_{min} is expressed as:

$$T_{min} = -1837.383 + 18.851 - 9.507I_b + 2495.127\rho - 21.917h_o - 0.839VoD - 2.425UCS \quad (7)$$

Analysis of the T_{min} model yielded several critical insights. B demonstrated an inverse relationship with T_{min}, consistent with its established role in blast mechanics. Increasing B makes it take more energy to move the rock, which extends the response duration. This discovery corresponds with previous investigations that have identified burden as a primary determinant. While Chiappetta [15], who first defined the term "rock's response time to blasting", suggested hole diameter influences T_{min}, this study confirms its role is meaningfully contextualized by considering the explosive type. More significant results emerged when incorporating I_b—a parameter functionally dependent on hole diameter and explosive density—rather than hole diameter alone. Higher I_b values improve the efficiency of energy transmission and can be attained with denser explosives or larger borehole diameters. Furthermore, increased VoD decreases T_{min}, confirming explosive properties as critical determinants. Previous research on the properties of rocks has shown mixed results regarding the impact of intrinsic material properties on T_{min}. This study clarifies this ambiguity by establishing clear directional effects: ρ shows a positive relationship with T_{min}, suggesting inertial resistance in denser m, while UCS shows a negative correlation with T_{min}, suggesting faster response in competent rock. This finding aligns with Bergmann's postulations [4]. Interestingly, h_o showed up as a new predictor; longer stems were linked to lower T_{min}. This indicates better energy confinement from a mechanistic standpoint, as gaseous products are directed toward rock fracturing instead of escaping to the atmosphere.

Equation (7) provides a practical engineering tool for optimizing delay timing based on site-specific geomechanical and explosive properties. Its incorporation of four controllable parameters (B, I_b, h_o, and VoD) positions T_{min} as a controllable variable rather than merely an observational outcome.

4.2. Rock-Size Reduction Ratio (F) Model

Given the critical influence of delay time on fragmentation outcomes, appropriate delay intervals are fundamentally dependent upon the T_{min}. This dependence establishes a direct correlation between T_{min} and fragmentation efficiency. To quantitatively characterize this relationship within the framework of temporally optimized blasting, the second regression model formalized F as the dependent variable. Based on a coefficient of determination (R^2 = 0.803), the model was very good at making predictions. Comprehensive model summary statistics are detailed in Table 8. Analysis of variance (ANOVA) results, presented in Table 9, confirmed the model's statistical significance at the 95% confidence level ($p < 0.001$). The accompanying coefficients table explicitly delineates the magnitude and directional contribution of each predictor variable.

Table 8. Model summary of rock-size reduction ratio (F) estimation.

Model	R	R Square	Adjusted R Square	Std. Error of the Estimate
1	0.896 [a]	0.803	0.786	1.24798

[a]. Predictors: (Constant), q, UCS, T_{min}, U.

Table 9. Analysis of variance for rock-size reduction ratio (F) estimation.

Model		Sum of Squares	df	Mean Square	F	Sig.
1	Regression	308.415	4	77.104	46.952	<0.001 [b]
	Residual	75.540	46	1.642		
	Total	383.955	50			

Coefficients [a]

Model		Unstandardized Coefficients		Standardized Coefficients	t	Sig.
		B	Std. Error	Beta		
1	(Constant)	87.389	1.385		63.094	0.000
	q (kg/m^3)	8.011	1.659	0.345	4.828	0.000
	UCS (MPa)	−0.035	0.007	−0.416	−4.686	0.001
	T_{min} (ms)	−0.022	0.006	−0.313	−3.840	0.005
	U (m)	1.442	0.228	0.497	6.317	0.000

[a] Dependent Variable: F (%). [b] Predictors: q (kg/m^3), UCS (MPa), T_{min} (ms), U (m).

The rock-size reduction ratio (F) equation is defined as:

$$F = 87.389 + 8.011q - 0.035UCS - 0.022T_{min} + 1.442U \quad (8)$$

To enhance practical utility, Equation (8) was reformulated to predict mean particle size (P_{50}) based on mean in situ block size (D_{50}):

$$P_{50} = D_{50} \times \left[1 - \frac{87.389 + 8.011q - 0.035UCS - 0.022T_{min} + 1.442U}{100}\right] \quad (9)$$

It can be said that the rock's response time to blasting has an inverse effect on rock fragmentation by blasting. This result, indicating an inverse relationship between the rock's response time and fragmentation, aligns with the findings of Voulgarakis et al. [26].

4.3. Validation

Model validation for Equation (9) utilized T_{min} values predicted by Equation (6), rather than direct field measurements. This approach tested the integrated model's reliability

under known design conditions. Figure 2 illustrates a strong correlation (R^2 = 0.837) between observed and predicted P_{50} values.

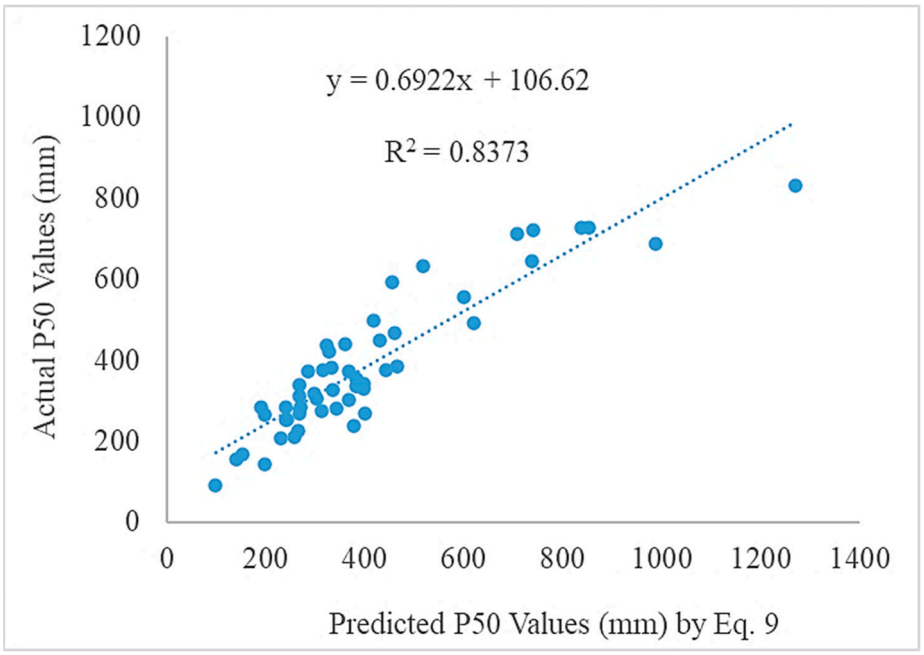


Figure 2. Correlation between actual P_{50} values and predicted P_{50} values by Equation (9).

The fragmentation model elucidates key mechanistic relationships. F increased with q and U, consistent with theoretical expectations. Conversely, F decreased with higher UCS and longer T_{min} values. Prolonged response time reducing fragmentation efficiency and increasing particle size. This positions T_{min} as a critical temporal determinant in fragmentation optimization, complementing traditional energy-based parameters. Crucially, the inverse relationship between F and T_{min} constitutes a novel empirical finding.

Model performance was further evaluated using multiple error metrics (Table 10). While high R^2 values confirm strong linear correlations, absolute error analysis provides complementary insight into predictive reliability.

Table 10. Accuracy assessment of the derived models.

Equation	Equation (7)	Equation (8)	Equation (9) *
Target	T_{min} (s)	F (%)	P_{50} (mm)
Minimum Error (%)	0.45	0.04	0.21
Maximum Error (%)	59.02	7.20	34.12
Mean Square Error (MSE)	357.32	7.93	2397.63
Mean Absolute Percentage Error (MAPE)	16.56	2.62	8.37
Root Mean Square Error (RMSE)	18.90	2.82	48.97
Correlation Coefficient (R^2)	0.789	0.803	0.837

* Rather than using the observed T_{min} values, estimated T_{min} values calculated by Equation (7) were used.

The developed models generally exhibit high reliability in predicting critical outcomes of blasting operations. The error rate for Equation (7) (T_{min} estimation) is less than 20% in 43 out of 51 examples; however, deviations are particularly pronounced in a few cases, including Data No. 8 (46.9%), 32 (59.0%), and 35 (51.0%). While Equation (7) generally performed with acceptable accuracy, significant error rates were observed in 3 of the 51 datasets.

Similarly, Equation (8) (F estimation) exhibits largely low errors (0.0–5.9%), with only Data No. 41 (7.1%) and 42 (7.2%) exhibiting exceptionally high deviations. Equation (9) (P_{50} estimation) achieves consistent performance with errors below 20% for 48 data, except for Data 19 (34.1%), 49 (25.5%), and 50 (19.2%). These outliers are anticipated to be the result of boundary design conditions or excessively high actual P_{50} values (e.g., 832 mm). While not all models exhibit mean absolute percentage errors (Equation (7): 16.56%, Equation (8): 2.62%, Equation (9): 8.37%) that surpass the industrial acceptance threshold (20% MAPE).

Samples containing high errors may be due to inaccuracies in measurement procedures, accidental factors, sudden drops in explosive performance, or local geotechnical heterogeneities. These kinds of deviations do not invalidate the general validity of the models. However, it must be emphasized that the aforementioned reasons are currently only speculative, as they have not yet been confirmed by direct empirical findings or conclusive field data.

4.4. Testing

A field testing was conducted in Study Field 7 to assess the practical utility of Equations (7)–(9) derived from regression analysis. The blasting pattern of the test shot is presented in Figure 3, and the values of predictors are presented in Table 11.

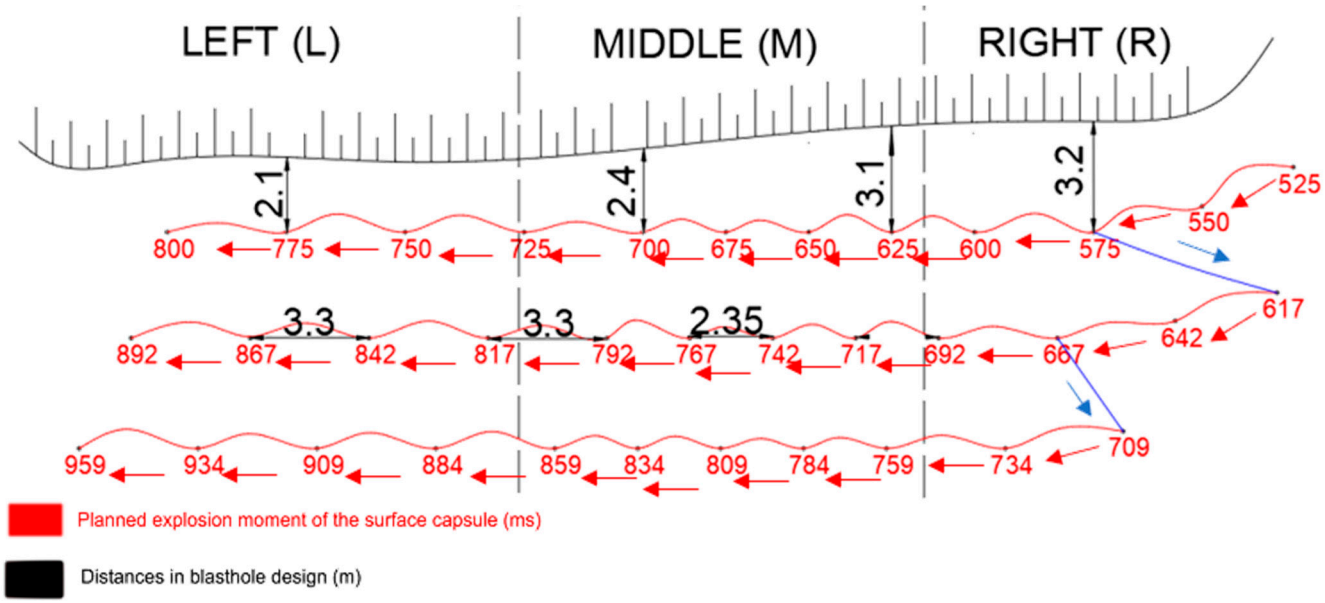
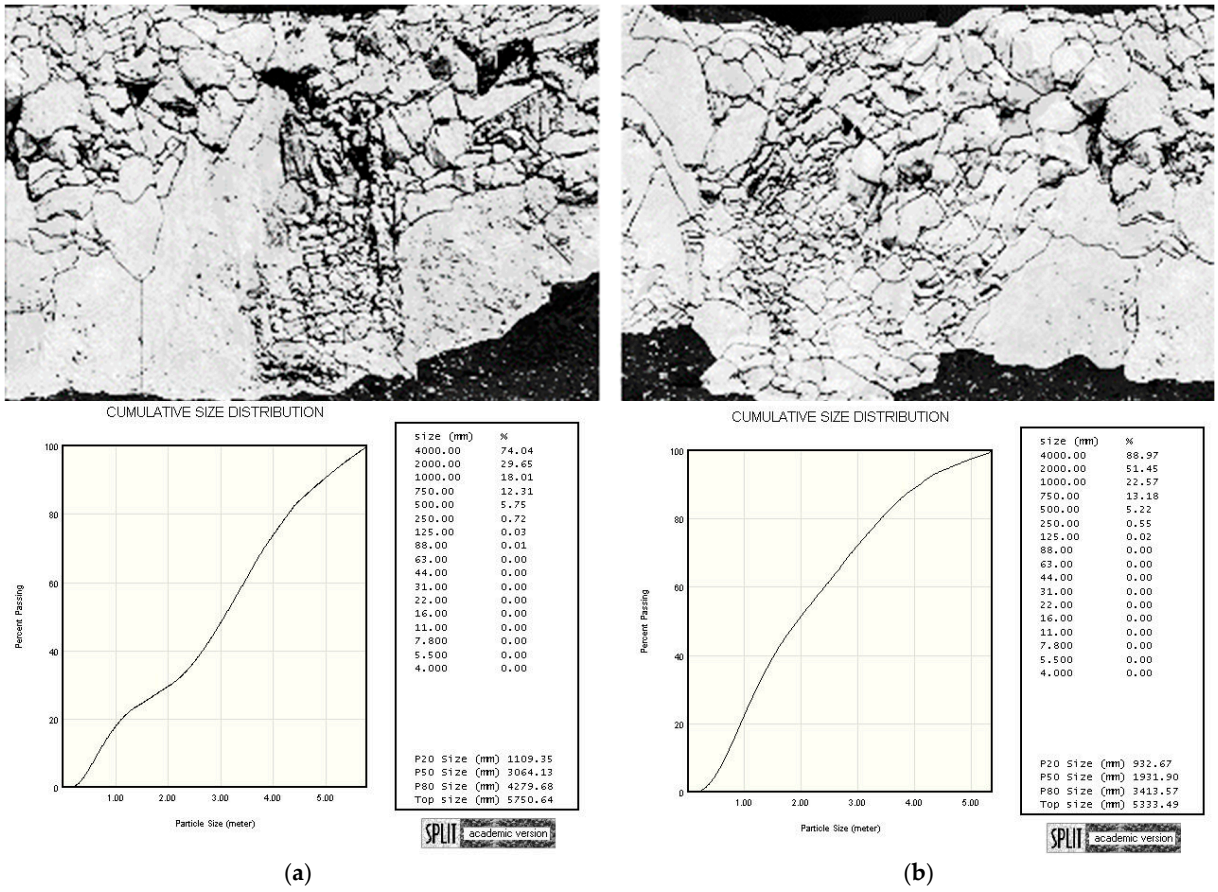


Figure 3. Blasting design parameters and timing details of the test shot.

Table 11. Blasting design parameters, pertinent charge specifications, and capsule details of the test shot.

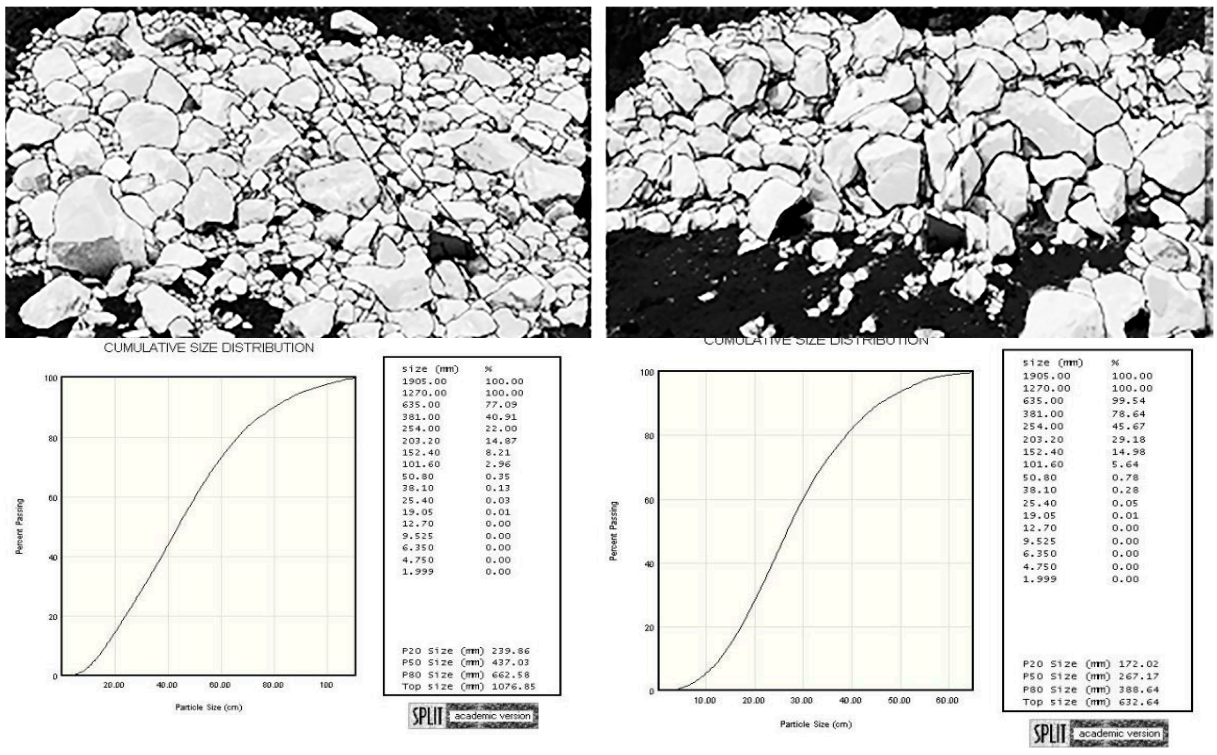
Field No	Zone	B_{max} (m)	S (m)	K (m)	d (mm)	Explosive	I_b (kg/m)	n	U (m)	H (m)	h_o (m)	VoD (m/s)	Q (kg)	q (kg/m^3)
7	Left	2.2	3.3	11	89	ANFO	4.97	11	1	12	2	4905	50.74	0.39
	Middle	3.1	2.35	11	89	ANFO	4.97	14	1	12	2	4905	50.74	0.49

Digital image processing was employed to determine the in situ block size and characterize the particle size distributions, as presented in Figures 4 and 5. The results indicate D_{50} of 3064 mm and a P_{50} of 437 mm in the left zone, the middle zone yielded a D_{50} of 1931 mm and a P_{50} of 267 mm. Furthermore, F was calculated to be 85.74% in the left zone and 86.16% in the middle zone.



(**a**) (**b**)

Figure 4. Digital image processing of (**a**) left (**b**) middle zone of bench face before test shot.



(**a**) (**b**)

Figure 5. Digital image processing of (**a**) left (**b**) middle zone of muck pile resulting from the test shot.

The high-speed camera recording showed that the time between the firing of the first surface capsule and the beginning of the rock movement in the middle zone was 717 milliseconds (Figure 6). In the left part, it took 691 milliseconds. In this shot, where Nonel capsules with 25 ms surface and 500 ms in-hole delays with a deviation of 16% were used, the response times of the rock to blasting were calculated as 79.96 ms for the left zone and 105.96 ms for the middle zone.



(**a**) t = 723 ms (**b**) t = 1414 ms

Figure 6. (**a**) The moment of the surface capsule fired, (**b**) The moment of rock movement began in the test shot.

Table 12 demonstrates a strong agreement between the developed models (Equations (7)–(9)) and field measurements, with consistently low prediction errors of less than 10%.

Table 12. Comparison of actual results and predicted values.

	Field Measures		**Predictions**		**Error (%)**	
Region	Left	Middle	Left	Middle	Left	Middle
T_{min} (ms)	79.96	105.96	85.17	102.13	6.5	3.6
F (%)	85.74	86.16	88.99	89.22	3.8	3.5
P_{50} (mm)	437	267	395	244	9.6	8.7

5. Results and Discussion

The study's results make a substantial contribution to the body of knowledge regarding the connection between fragmentation efficiency and T_{min}.

The primary engineering contribution of this study lies in the development of a comprehensive and integrated model for predicting blast performance. In contrast to the existing literature, this research extends beyond predicting the response time of rocks to blasting (T_{min}) (R^2 = 0.789) by utilizing this predicted value as a direct input to sequentially estimate fragmentation performance (F, % $-$ R^2 = 0.803) and ultimately the mean fragment size (P_{50} $-$ R^2 = 0.837). This study is the first to directly integrate the prediction of T_{min} with the estimation of P_{50}, thereby establishing a continuous and holistic predictive model.

One of the original contributions of this study is its revelation of the effect of h_o on T_{min}. The finding that longer stemming is associated with shorter T_{min} provides a significant contribution to understanding the mechanism of energy confinement. This can be explained by the fact that longer stemming confines a much larger portion of the high-temperature and high-pressure gases, which are crucial for rock fragmentation upon detonation, within the blast hole. This confinement facilitates easier and faster rock fragmentation, thereby resulting in a shorter T_{min}. Furthermore, another important contribution is the expansion

of Chiappetta's [8] emphasis on hole diameter by incorporating I_b, which depends on both hole diameter and explosive density, thus offering a more comprehensive approach.

The study's conclusions about the effects of the parameters on T_{min} exhibit both notable parallels and divergences with previous research. First, all researchers on this topic agree that B and T_{min} have an inverse relationship. Similarly, the critical role of explosive properties parallels the concept of Explosive–Rock Interaction (*ERI*) emphasized by Onederra and Esen [22]. Also, this study shows that increasing *VoD* greatly lowers T_{min}. This supports the ideas put forward by Onederra and Esen [22].

This study clarifies the uncertainties in the literature regarding the effect of rock properties. A positive correlation was observed between T_{min} and ρ. Furthermore, the negative correlation between *UCS* and T_{min} provides experimental confirmation for Onederra and Esen's [22] emphasis on rock hardness. However, this finding is not consistent with the assertion by Segarra et al. [23] that rock type has no effect. Overall, these results demonstrate that rock properties have a significant impact on T_{min}.

To demonstrate the impact of T_{min} on fragmentation, the developed model (Equation (9)) was applied to the whole range of response time values measured during the study (30–185 ms) while preserving the mean parameter values from the current dataset (q: 0.44 kg/m^3, *UCS*: 98 MPa, *U*: 0.68 m, and D_{50}: 3035 mm). The findings indicated that the P_{50} value was estimated at 370 mm (F = 87.80%) at the lower limit response time of 30 ms and at 474 mm (F = 84.39%) at the upper limit response time of 185 ms. These results demonstrate that P_{50} increased significantly by 28.1% when T_{min} was increased by about six times (6.17×). This result validates that longer response has a significant negative impact on fragmentation efficiency, a finding that aligns with the core relationship between timing and fragmentation outcomes explored by Voulgarakis et al. [26].

This negative impact of the T_{min} of fragmentation can be explained based on the theoretical framework concerning the fragmentation mechanism. The first and most important possibility is that the high-pressure and high-temperature gases formed as a result of the detonation may not maintain their pressure and drop before fragmentation is complete. According to theory, the ability of these high-energy gases to propagate through existing discontinuities within the rock is due to the high pressure they possess. An increase in the rock's response time to blasting likely means this process will progress more slowly. According to the predicted scenario, this delay could allow the gases to escape early from the borehole, seep into pre-existing crack intervals, or expand, cool down, and lose their critical pressure levels. It can be proposed as a probable outcome that gases with reduced pressure cannot transfer sufficient energy to the crack tips, and crack propagation is halted prematurely. This situation is expected to result in insufficient fragmentation and larger blocks. A second possible explanation is the disruption of the timing and synchronization between the sequential stages assumed to be necessary for effective fragmentation. According to theoretical models, the timing between the shock wave creating micro-cracks in the rock and the gases expanding and extending these cracks should be near optimal. It is predicted that a long response time may cause a timing discrepancy by creating a disadvantage between these two critical stages. It is likely that by the time the gases reach the crack zones, the effect of the shock wave may have already diminished, or the crack tips may no longer be amenable to propagation.

Building upon this relationship between timing and fragmentation, a comparative analysis was conducted between the model developed in this study and the approach proposed by Voulgarakis et al. [26] (Figure 7), which also explicitly relates F to T_{min}. However, a critical limitation of the model by Voulgarakis et al. [26] (Equation (4)) emerges as the fragmentation process becomes more efficient: when the mean in situ block size exceeds 7.116 times the mean particle size (corresponding to a fragmentation ratio, F,

exceeding 85.95%), the predicted T_{min} value approaches infinity. Since modern quarry operations target high fragmentation values (typically between 83.02% and 96.47%), the model developed in this study demonstrates superior and practical performance within this critical range. A comparison of 26 data points where both models are applicable (F < 85.95%) revealed that Equation (7) from this study achieved a Mean Absolute Percentage Error (MAPE) of 18.90, significantly lower than the MAPE of 54.26 for Equation (4) from Voulgarakis et al. [26]. These results underscore that the current study provides an alternative tool with high applicability in the high-efficiency fragmentation range demanded by industry.

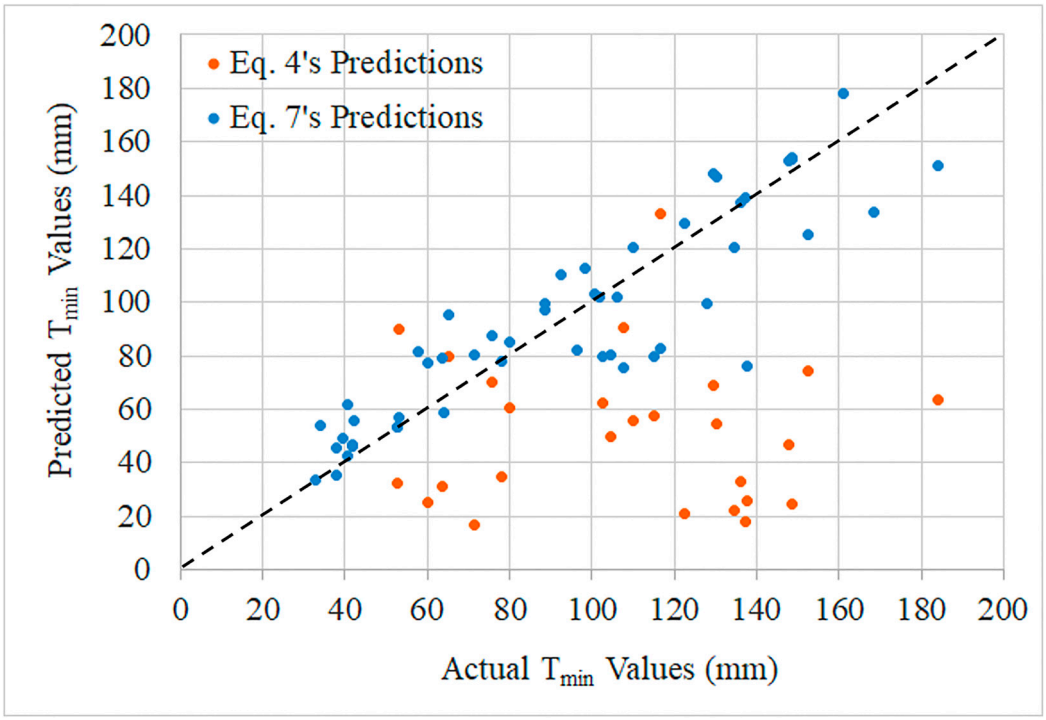


Figure 7. Comparison of the actual T_{min} values and predicted T_{min} values by Equations (4) and (7).

While Onederra and Esen's model [22] is theoretically valuable, its reliance on complex parameters (e.g., ERI, K_{mass}, E_r) often makes it impractical for field measurements. In contrast, the models developed in this study utilize readily available parameters, making them significantly more user-friendly for engineering applications. This enhanced practicality provides engineers with a more viable and efficient tool for use in the field.

The proposal by Chiappetta [8], who introduced the concept of T_{min} to the literature, has been re-evaluated in light of the dataset generated in this study. Chiappetta suggested that the inter-row delay time should be 1.5–3 times T_{min}. However, the ratio was observed to vary between 0.5 and 5.9. Interestingly, although the number of data points falling within Chiappetta's proposed range was relatively limited (16 data points), no statistically significant difference in fragmentation performance was observed across the different ratio intervals (0.5–1.5, 1.5–3, and 3–5.9). Nevertheless, the dataset's exceptionally fine post-blast particle sizes and the notably high F imply that the specific charge values applied may have been significantly greater than the energy necessary to fragment the respective rock masses. The use of such high specific charge values may have masked the potential effects of Chiappetta's proposed optimal delay interval, preventing its validation under these conditions. Thus, more research examining the viability of Chiappetta's suggestion under more regulated blasting circumstances with an optimized specific charge is necessary and would be beneficial to the field.

6. Conclusions

This study presents a novel methodology for the estimation of T_{min}, a critical parameter that directly affects fragmentation efficiency in blasting operations. Unlike the existing literature, this study not only estimated T_{min} but also used this parameter as a direct input in an integrated model that sequentially predicts fragmentation performance (F, %) and mean fragment size (P_{50}). The developed model offers a quantitative improvement compared to existing practical models, with high prediction accuracy (R^2 = 0.789 for T_{min}, R^2 = 0.803 for F, R^2 = 0.837 for P_{50}) and low error rates (MAPE: 16.56% and 2.62%, respectively), constituting a more reliable and applicable alternative within the industry's high-efficiency range (F > 83.02%).

The experimental results of the study clearly showed that T_{min} is an optimizable variable through controllable parameters such as blasting design and proper explosive selection. Specifically, the determining effect of design parameters like burden and stemming length, as well as rock properties like velocity of detonation and rock's unit volume weight and uniaxial compressive strength on T_{min}, was modeled. One of the most important findings is the first-time demonstration that longer stemming reduces T_{min} by increasing energy confinement. Furthermore, it was experimentally proven that a 6.17× increase in T_{min} leads to a significant 28% increase in P_{50}, quantitatively demonstrating the negative impact of long response times on fragmentation efficiency.

The primary engineering contribution of this study is that it presents an integrated prediction model that transforms theoretical complexity into practical applicability, using parameters that can be easily measured or controlled in field conditions. It provides engineers with a practical tool to achieve better fragmentation quality and operational cost advantages by optimizing the timing of the interaction between blasting energy and the rock mass.

A limitation of the study is that, although the experimental data range is consistent with the framework of established blasting guides recommended by authorities such as Langefors and Kihlström [36], Olofsson [37], and Jimeno et al. [5], the validation of the model needs to be tested in different geological environments and wider parameter ranges.

In conclusion, this research paves the way for more efficient, controlled, and optimized blasting practices by highlighting the critical role of T_{min} on fragmentation performance. In light of these findings, the following directions are suggested for future research:

1. Advanced geological mapping in each rock mass should be carried out to identify rock mass anomalies (intense fracture/jointed zones, voids, etc.) that are difficult to detect with ordinary and classical methods. It will enable the development of new approaches that increase T_{min} prediction accuracy. In this context, the goal is to investigate the direct effect of discontinuities on T_{min} with increasing R^2 and decreasing MAPE values.
2. Future research should focus on integrating the prediction equations for T_{min} and F developed in this study into blasting simulation software and optimization algorithms. By inverting these models, the optimal blasting design parameters—such as burden, spacing, specific charge, and stemming length—could be predicted to achieve a targeted fragmentation distribution and post-blasting particle size. It is recommended that such tools be developed to bridge the gap between predictive modeling and operational design, allowing for the optimization of blast parameters and explosive selection based on specific rock mass behavior.
3. Unlike this study, it should be planned to quantify the relationship between inter-row delay time and T_{min} for optimal fragmentation in scenarios where the specific charge is optimized for a larger but still acceptable particle size. This study will significantly contribute to understanding the practical validity of the range proposed by Chiappetta [8].

Author Contributions: M.C.O. (First Author) and A.K. (Corresponding Author) were integrally involved in all aspects of the research, including study conceptualization, methodological development, data acquisition and analysis, and manuscript preparation. U.K.S. and U.O. made significant contributions to the methodological framework and analytical approach. The field-based investigations—encompassing geological characterization, blast parameter quantification, and photogrammetric/videogrammetric assessments—were primarily conducted by H.E.M. and T.C.O., whereas U.K.S. performed the statistical analyses. All authors contributed substantially to data interpretation, participated actively in the drafting and critical revision of the manuscript, and approved the final version for publication. U.O. provided academic supervision and was responsible for funding acquisition. All authors have read and agreed to the published version of the manuscript.

Funding: This work was financially supported by the Scientific and Technological Research Council of Türkiye (Projects: "Evaluation of Blasting Excavation Works Carried Out In The Thrace Region in Terms of Efficiency" and "Investigation of Response Times and Behaviors of Rocks to Blasting, 120M421").

Data Availability Statement: The data presented in this study are available on request from the corresponding author due to their ongoing use in further research.

Acknowledgments: The authors would like to thank the Scientific and Technological Research Council of Türkiye (Tübitak), Abdulkadir ARSLAN from Ento Mining Construction Industry & Trade LLC Co., Ünal GÜNDÜZ from NITRONET and Cevdet Burkay ZAIF from Nobel Explosives.

Conflicts of Interest: Author Hilal Erem Mutlu was employed by the company Tessan Mining Construction Industry Tourism and Trade Joint Stock Company. Author Taki Can Odabasi was employed by the company Erdemir Mining Industry and Trade Inc. The remaining authors declare that the research was conducted in the absence of any commercial or financial relationships that could be construed as a potential conflict of interest.

References

1. Ash, R.L. *The Design of Blasting Rounds, Surface Mining*; Pfleider, E.P., Ed.; The American Institute of Mining, Metallurgical, and Petroleum Engineers: New York, NY, USA, 1968; pp. 373–397.
2. Hagan, T.N.; Cameron, A.R. Selecting Explosives Systems and Monitoring Their Performance in Surface Mines. In *Mine Planing and Equipment Selection*; Pasamehmetoglu, A.G., Eskikaya, S., Karpuz, C., Hizal, T., Eds.; Balkema: Rotterdam, The Netherlands, 1994; pp. 635–641.
3. Fourney, W.L. *Mechanism of Rock Fragmentation by Blasting, Comprehensive Rock Engineering*; Hudson, J.A., Ed.; Pergamon Press: Oxford, UK, 1993; Volume 4, pp. 39–69.
4. Petrosyan, M.I. *Rock Breakage by Blasting*; A.A. Balkema: Rotterdam, The Netherlands, 1994; 141p.
5. Jimeno, L.C.; Jimeno, E.L.; Carcade, F.J.A. *Drilling and Blasting of Rock*; A.A. Balkerna: Rotterdam, The Netherlands, 1995.
6. Borovikov, V.A.; Vanyagin, I.F. *Modelling the Effects of Blasting on Rock Breakage*; A.A. Balkema: Rotterdam, The Netherlands, 1995; 238p.
7. Djardjevic, N. A Two-Component Model of Blast Fragmentation. *AusIMM Proc.* **1999**, *304*, 9–13.
8. Chiappetta, R.F. Blast Monitoring Instrumentation and Analysis Techniques, with an Emphasis on Field Applications. *FRAGBLAST-Int. J. Blasting Fragm.* **1998**, *2*, 79–122. [CrossRef]
9. Bauer, A.; Calder, P.N. *Open Pit and Blasting*; Seminar Mining Engg. Dept. Publication; Queen's University: Kingston, ON, USA, 1970; p. 3.
10. Bergmann, O.R.; Wu, F.C.; Edl, J.W. Model rock blasting measures effects of delays and hole patterns on rock fragmentation. *Engng. Min. J.* **1974**, *175*, 124–127. [CrossRef]
11. Winzer, S.R.; Anderson, D.A.; Ritter, A.P. Rock Fragmentation by Explosives. In Proceedings of the First International Symposium on Rock Fragmentation by Blasting, Lulea, Sweden, 23–26 August 1983; pp. 225–249.
12. Bergmann, O.R. Effect of explosive properties, rock type and delays on fragmentation in large model blasts. In Proceedings of the First International Symposium on Rock Fragmentation by Blasting, Lulea, Sweden, 23–26 August 1983; pp. 71–78.
13. Fadeev, A.B.; Glosman, L.M.; Kartuzov, M.I.; Safonov, L.V. Seismic control of mine and quarry blasting in the USSR. In Proceedings of the 6th Congress of the International Society for Rock Mechanics, Montreal, QC, Canada, 30 August–4 September 1987; International Society for Rock Mechanics: Montreal, QC, Canada, 1987; pp. 617–619.

14. Andrews, A.B.S. Design criteria for sequential blasting. In Proceedings of the Seventh Conference on Explosives and Blasting Technique, Phoenix, AZ, USA, 12–23 January 1981; Society of Explosives Engineers: Warrensville Heights, OH, USA, 1981; pp. 173–192.
15. Stagg, M.S.; Rholl, S.A. Effects of accurate delays on fragmentation for single-row blasting in a 6.7m (22ft) bench. In Proceedings of the Second International Symposium on Rock Fragmentation by Blasting, Keystone, CO, USA, 23–26 August 1987; pp. 210–230.
16. Stagg, M.S.; Nutting, M.J. *Influence of Blast Delay Time on Rock Fragmentation: One-Tenth-Scale Tests*; US. Bureau of Mines IC 9135: Minneapolis, MN, USA, 1987; pp. 79–95.
17. Konya, C.J.; Walter, E.J. *Surface Blast Design Englewood Cliffs*; Prentice Hall, Inc.: Englewood Cliffs, NJ, USA, 1990.
18. McKinstry, R.; Bolles, T.; Rantapaa. Implementation of Electronic Detonators at Barrick Goldstike Mines. In Proceedings of the 30th ISEE Annual Conference on Explosives and Blasting Technique, New Orleans, LA, USA, 1–4 February 2004; Volume 1, pp. 349–361.
19. Otterness, R.E.; Stagg, M.S.; Rholl, S.A.; Smith, N.S. Correlation of shot design parameters to fragmentation. In Proceedings of the 7th Annual Symposium on Explosives and Blasting Technology, Las Vegas, NV, USA, 6–7 February 1991; International Society of Explosives Engineers (ISEE): Cleveland, OH, USA, 1991; pp. 179–190.
20. Chung, S.; Katsabanis, P.D. An Integrated Approach for Estimation of Fragmentation. In Proceedings of the 27th ISEE Annual Conference on Explosives and Blasting Technique, Orlando, FL, USA, 28–31 January 2001; Volume 1, pp. 247–256.
21. Katsabanis, P.D.; Tawadrous, A.; Braun, C.; Kennedy, C. Timing effects on the fragmentation of small scale blocks of granodiorite. *Fragblast* **2006**, *10*, 83–93. [CrossRef]
22. Onederra, I.; Esen, S. Selection of inter hole and inter row timing for surface blasting- an approach based on burden relief analysis. In Proceedings of the EFEE Second World Conference on Explosives and Blasting Technique, Prague, Czech Republic, 10–12 September 2003; Swets and Zeitlinger: Lisse, The Netherlands, 2003.
23. Segarra, P.; Sanchidrián, J.A.; López, L.; Pascual, J.A.; Ortiz, R.; Gómez, A.; Smoech, B. Analysis of bench face movement in quarry blasting. In Proceedings of the Second World Conference on Explosives and Blasting Technique, Prague, Czech Republic, 10–12 September 2003; Holmberg, R., Ed.; Balkema: Rotterdam, The Netherlands, 2003; pp. 485–495.
24. Sanchidrián, J.A.; Segarra, P.; López, L.M. On the relation of rock face response time and initial velocity with blasting parameters Brighton Conference Proceedings. In Proceedings of the 3rd EFEE World Conference on Explosives and Blasting, Brighton, UK, 14–16 September 2005; European Federation of Explosives Engineers: Kraków, Poland, 2005; ISBN 0-9550290-0-7.
25. Onederra, I. Delay timing factor for empirical fragmentation models. *Min. Technol.* **2007**, *116*, 176–179. [CrossRef]
26. Voulgarakis, A.G.; Michalakopoulos, T.N.; Panagiotou, G.N. The minimum response time in rock blasting: A dimensional analysis of full-scale experimental data. *Min. Technol.* **2016**, *125*, 242–248. [CrossRef]
27. Sunnetcioglu, M.A. A Sequence Stratigraphic Approach to the Depositional History Analysis of the Upper Eocene Sedimentary Succession, Northwest of the Thrace Basin, Turkey. Ph.D. Thesis, Middle East Technical University, Ankara, Türkiye, 2008.
28. Yurtsever, A. *1/200.000 Scale Exploratory Thrace Geological Map Promotion Report*; MTA Arts & Design: Istanbul, Turkey, 1996; 52p.
29. Guler, O.; İskan, B. *Kırklareli Province–Vize District–Evrencik Village, TRAÇİM Çimento San. And Trade. Inc. Vize Cement Factory Geological and Hydrogeological Research of Mining License Areas (IR 64145, IR 20062296, IR 20062297, IR 20062298) and their Surroundings*; Technical Report; Environmental Laboratory, Artek Engineering, Environmental Measurement and Consulting Services Trade Inc.: Vize, Turkey, 2021. (In Turkish)
30. Uz, B. *Study and Evaluation Report of the Geological/Structural, Mineralogical-Petrographical and Physico-Mechanical Properties of the Crushed Stone Quarry of Akdağlar Madencilik A.Ş*; Ayazağa Village Cendere Locality, ITU Mining Faculty Geological Engineering Department, Mineralogy Pertography Department: Istanbul, Turkey, 2007. (In Turkish)
31. Keskin, C. Geology of the Pınarhisar Area. *Türkiye Jeol. Bülteni* **1971**, *14*, 31–83. (In Turkish)
32. Uçankuş, T.; Koyuncu, F.T.; Göveli, A.; Büyüktanir, S.A.; Taştan, F.; Dursun, K. *Limak Batı Cement San. ve Tic. A.S. Limestone Quarry, License No 200901722, Final EIA Report*; Ankatek Çevre Mad. Eng. Co.: Ankara, Turkey, 2014. (In Turkish)
33. Atalık, E. Depositional Systems of the Osmancık Formation in the Thrace Basin: METU. Ph.D. Thesis, The Graduate School of Natural and Applied Sciences, Atasehir, Turkey, 1992; 366p.
34. Atalık, E. *Thrace Basin Soğucak Formation Sedimentary Environments and Microfacies Analysis: TPAO Exploration Group Archive*; Unpublished Technical Report, no: 2305; 1987; 92p.
35. Celikkurt, K.C. The Sedimentology of Coal and Uranium Bearing Sequences in the Saray and Vize Area. Master's Thesis, Istanbul University-Cerrahpasa, Institute of Graduate Studies, Department of Geological Engineering, Istanbul, Türkiye, 2020.

36. Langefors, U.; Kihlström, B. *The Modern Technique of Rock Blasting*, 2nd ed.; John Wiley & Sons: Hoboken, NJ, USA, 1962; ISBN 10: 047151571X; ISBN 13: 9780471515715.
37. Olofsson, S.O. *Applied Explosives Technology for Construction and Mining*, 2nd ed.; Applex: Arla, Sweden, 1988.

Disclaimer/Publisher's Note: The statements, opinions and data contained in all publications are solely those of the individual author(s) and contributor(s) and not of MDPI and/or the editor(s). MDPI and/or the editor(s) disclaim responsibility for any injury to people or property resulting from any ideas, methods, instructions or products referred to in the content.